



Propene induced reversible deactivation effects in diesel oxidation catalysts



M. Herrmann^{a,b}, R.E. Hayes^c, M. Votsmeier^{a,*}

^a Umicore AG & Co. KG, Hanau-Wolfgang, D-63403, Germany

^b Ernst-Berl-Institut, Technische Universität Darmstadt, Darmstadt, D-64287, Germany

^c Department of Chemical and Materials Eng., University of Alberta, Edmonton, AB T6G 2V4, Canada

ARTICLE INFO

Article history:

Received 10 April 2017

Received in revised form 26 July 2017

Accepted 6 August 2017

Available online 12 August 2017

Keywords:

Activation

Deactivation

DOC

Pt/Pd catalyst

Propene

ABSTRACT

By applying different transient test protocols in a lab reactor, it is demonstrated that in the presence of C_3H_6 a Pt/Pd based oxidation catalyst experiences a persistent deactivation that can be attributed to the accumulation of propene partial oxidation products on the catalyst surface. The deactivation can be reversed by treating the catalyst at higher temperature in a hydrocarbon free atmosphere. The three most important scenarios giving rise to the activation/deactivation phenomenon are:

(1) Consecutive heat-up/cool-down cycles: If several consecutive heat-up/cool-down cycles are performed with a catalyst pretreated in a propene free oxidative atmosphere, a lower ignition temperature is observed during the first heating ramp than during the following cycles. The effect can be explained by a reversible blocking of active sites by hydrocarbon (HC) intermediates, which are formed during the ignition branch, then entirely are removed after the HC ignition is completed and finally are formed again during the extinction branch, providing a deactivated state of the catalyst for the following ignition. The deactivation can be completely reversed either by a conditioning in an oxidizing HC free gas mixture at temperatures above 110 °C or a conditioning in N_2 above 140 °C. The deactivation effect is more pronounced under conditions that lead to a low light-off temperature and completely disappears at conditions leading to higher light-off temperatures, i.e. high CO concentrations or high space velocities.

(2) Light-off tests with varying temperature ramp rate: For faster ramp rates, CO/propene ignition is observed at lower inlet temperatures. This is the opposite behavior than would be expected based on thermal considerations and can be explained by a higher accumulation of HC intermediates during the slower ramp.

(3) Transient observation of the deactivation effect: If an initially clean catalyst is operated at a constant temperature in the light-off range, a transient decrease in CO/HC conversion is observed that can be attributed to the gradual build-up of the blocking HC intermediates.

A kinetic model is presented which considers not only the standard CO and hydrocarbon oxidation kinetics, but also the formation of site blocking intermediates by partial oxidation of propene and the removal of these blocking intermediates either by total oxidation with O_2 or by thermal desorption. The model nearly quantitatively reproduces the experimental results of the different test protocols.

© 2017 Elsevier B.V. All rights reserved.

1. Introduction

The diesel oxidation catalyst (DOC) is a key component in diesel exhaust gas aftertreatment systems for the oxidation of hydrocarbons (HC) and CO as well as for the conversion of NO to a desired NO_2/NO ratio. Typical catalysts are Pt or a combination of Pt and Pd [1,2].

It has been reported [3–10] that under typical exhaust treatment operating conditions reversible activation and deactivation, as well as irreversible deactivation effects can be observed. This artifact poses a fundamental challenge for the assessment of the catalyst performance as well as for the application of global kinetic models in reactor simulations. Global kinetic models are usually empirical and have a form similar to the Langmuir-Hinshelwood-Hougen-Watson (LHHW) rate expressions (although they are not derived using the classical LHHW approach) [11]. For comparisons of different catalyst technologies, as well as for the parametrization of global kinetic models, steady state experiments (or very slow

* Corresponding author.

E-mail address: votsmeier@eu.umicore.com (M. Votsmeier).

transient ones) are typically applied [1,2,12,13]. Both procedures rely on the assumption that the rates of the surface reactions are only controlled by competition for surface sites and that steady state surface concentrations are instantly established for given gas phase conditions [14,15]. Thus global rate laws can be formulated and catalytic performance can be assessed as a function of only the current gas phase concentrations and the surface temperature, and not the recent history of operating conditions.

One prominent example for such a reversible activation/deactivation effect is the inverse hysteresis during NO oxidation investigated by Hauptmann et al. [5] on a Pt catalyst. The effect was explained as a reversible oxidation of the catalyst surface by NO₂ or O₂ at higher temperatures and a reduction of the oxides by NO at lower temperatures. The inverse hysteresis effect has been investigated in more detail in a number of studies [6–9] and can be reproduced by global [7,9] as well as by microkinetic models [5] for simple gas mixtures.

Dubbe et al. [9] recently reported, apart from the inverse NO hysteresis on platinum, further deactivation and reactivation effects in CO, NO and C₃H₆ conversion on platinum as well as on palladium catalysts which were attributed to a reversible oxidation/reduction of the precious metal.

The practical relevance of such reversible activation/deactivation effects has been highlighted by Bantl-Konrad et al. [15] and Arvajová et al. [10] for the adjustment of an optimal NO/NO₂ ratio.

Investigating the oxidation of CO/C₃H₆ mixtures during a single ignition/extinction experiment, Abedi et al. [16] observed a switch from a normal to an inverse hysteresis with decreasing CO/C₃H₆ ratio. By using DRIFT-spectroscopy on Pt/Al₂O₃ powder samples to analyze surface species, the effect was attributed to the formation of HC residuals competing with other pollutants for active sites. Herrmann et al. [14] extended the work of Abedi et al., and measured the CO and C₃H₆ conversion during consecutive ignition extinction experiments on a similar catalyst. They concluded that the inverse hysteresis observed by Abedi et al. was not, in fact, a hysteresis effect but rather a permanent deactivation which could be reversed by a temperature ramp up to 350 °C in a flowing gas without pollutants. Hazlet and Eppling reported that in gas mixtures containing CO and propene after the initial onset of CO conversion a plateau in the CO light-off curve is observed before full conversion is reached at higher temperatures [17]. It was shown by DRIFTS experiments that this observation can also be explained by an inhibition of the catalyst by partial oxidation products of propene [17,18].

In this work we investigate the deactivation and reactivation effects of a Pt/Pd catalyst in greater detail than were investigated on the Pt catalysts. Therefore we perform consecutive ignition extinction experiments, show for which temperature range of the heat-up/cool-down sequence HC intermediates are formed and removed, and investigate which temperatures are necessary to reactivate the catalyst either in oxidative gas mixtures free of pollutants due to reaction or in N₂ due to desorption of HC intermediates. Besides this, we demonstrate that the applied heating ramp of an ignition experiment significantly effects the conversion curves, corresponding to different degrees of deactivation, and make statements about various deactivation states obtained under different reaction conditions.

Finally, a macro kinetic single channel model that takes into account the formation and removal of HC intermediates is formulated. The purpose of the modeling work is to show that the observed deactivation phenomenon can be quantitatively explained by the assumption of the formation and the removal of HC intermediates during the ignition extinction cycle and to illustrate the effects.

2. Materials and methods

2.1. Experimental

2.1.1. Catalyst and reactor

A monolithic Pt/Pd diesel oxidation catalyst (length: 7.62 cm, diameter: 2.54 cm, 400 cpsi, 4 mil (0.1016 mm) wall thickness, hydrothermally aged (750 °C for 5 h), noble metal loading 125 g/ft³, Pt/Pd ratio 3:1 (kg/kg)) was used for all experiments. The monolith was wrapped with insulation and placed in a stainless steel tubular reactor taking care to ensure that no gas bypass of the monolith occurred.

2.1.2. Apparatus

The flow system consisted of a gas mixing unit, a gas pre-heater with the reactor and an analyzer module. Mass flow controllers were used to control and monitor the flow rate of each gas species. For experiments with water, steam was dosed to the feed using an evaporator system. Before passing through the monolith the gas mixture was heated in a tubular furnace. To ensure a uniform temperature profile and to enhance mixing of the gases, static mixers were installed in the oven. A k-type thermocouple was placed 1.5 cm in front of the catalyst entrance to monitor temperature.

2.1.3. Analyzer

NO and NO_x at the reactor outlet were analyzed using a chemiluminescence detector (CLD) and a flame ionization detector (FID) was used for the hydrocarbons assay. A paramagnetic method (MLT) was utilized to monitor O₂, while CO and CO₂ were analyzed applying a non-dispersive infrared sensor (NDIR).

2.1.4. Pretreatment

Before each experiment was performed the catalyst was treated with a defined mixture of inert gas species (10 % CO₂, 10 % H₂O, 10 % O₂, N₂ balance gas) while a temperature ramp from 75 to 400 °C and then back to 75 °C with a heating rate of 40 K/min and a cooling rate of –20 K/min was employed. The holding time at 400 °C was 5 min.

2.1.5. Ignition/extinction experiments

After the pretreatment, several ignition-extinction (IE) experiments were performed. The preheated gas stream with the inert gas species (10 % O₂, 10 % CO₂ and 10 % H₂O, N₂ balance gas) was mixed with a defined amount of noxious gases at a defined GHSV (STP) before reaching the catalyst. The ramp's maximum temperature is mentioned in the figure captions. The applied noxious gas concentrations, the ramp rates as well as the space velocities are reported in Table 1 for all types of experiments.

2.2. Simulation

Simulations were performed with a model that solves the heat and mass balance equations for a single catalyst channel. The balance equations for the gas phase were solved in terms of velocity averaged concentrations and temperature. Heat and mass transfer from the gas phase to the wall were described by heat and mass transfer coefficients computed from a Nusselt number correlation. Diffusion resistances in the washcoat were not explicitly solved for so that they are implicitly contained in the kinetic parameters. A detailed description if the applied simulation model can be found in Hauptmann et al. [19].

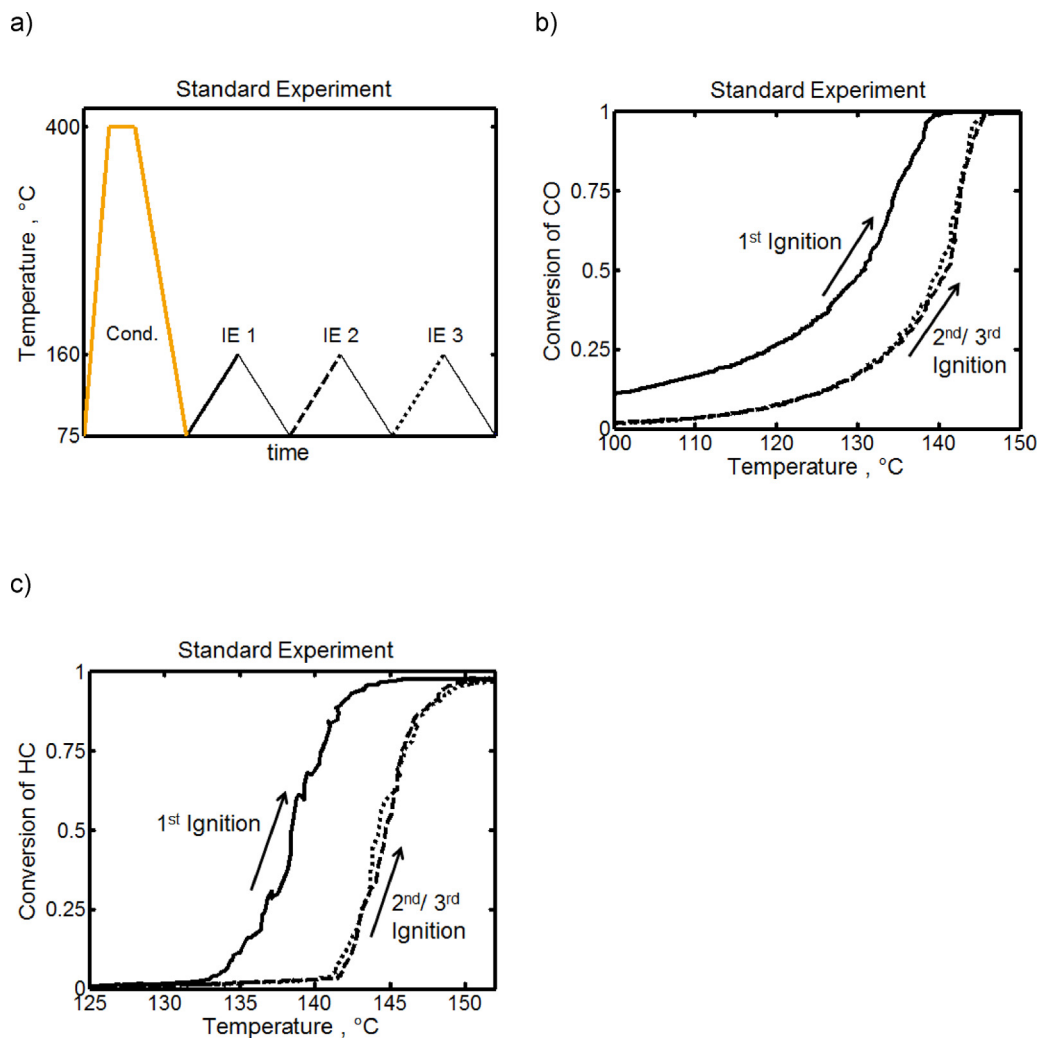


Fig. 1. Comparison of three CO and C₃H₆ ignition curves recorded during three ignition extinction cycles under standard conditions to show the catalyst's deactivation behavior. A schematic temperature ramp for the experiments preceded by a conditioning phase in an oxidative environment is shown in a). b) and c) represent the CO and the C₃H₆ ignition curves.

3. Results and discussion

3.1. Demonstration of the basic deactivation phenomenon

In the first experiment, three consecutive ignition extinction experiments were carried out using the temperature ramp scheme shown in Fig. 1a). The ramps represent the conditioning ramp and the three subsequent ignition extinction experiments.

The ignition curves for the three experiments are shown in the Fig. 1b) and c) for the conversion of CO and C₃H₆ respectively. It can be seen from these figures that the ignition curves for the second and third experiments coincide and are shifted to higher temperatures. Thus 10 °C and 7 °C higher temperature are required to reach 50% CO and 50% C₃H₆ conversion during the second and third ignition compared to the first one.

We have observed this deactivation effect previously on a Pt-catalyst and attributed it to the formation of C₃H₆ intermediates blocking active sites of the catalyst [14]. A catalyst deactivation during DOC light-off due to hydrocarbon intermediates was first proposed by Abedi et al. [16] who performed a single ignition extinction experiment on a Pt catalyst and observed a change from a normal to an inverse hysteresis with increasing C₃H₆/CO ratio. Using DRIFT-spectroscopy, they detected HC residuals on the catalyst's surface which could explain the lower activity during the

cool-down. In contrast to the Pt catalysts investigated in the previous studies, the Pt/Pd catalyst applied in this work does not show an inverse hysteresis (see Fig. S1 Supplementary).

3.2. Is the deactivation really HC induced?

To prove that the observed deactivation is caused by C₃H₆ in the feed, the ignition/extinction experiments of Fig. 1 were repeated without C₃H₆ in the feed. Experiments without NO and without either NO and C₃H₆ were also performed. The required temperatures for 50 % CO conversion during all ignition branches of the experiments are presented in Table 2, the light-off curves are shown in Fig. S2 of the Supplementary material.

It can be seen from the CO ignition temperatures that no deactivation occurs in the absence of C₃H₆, i.e. identical light-off temperatures are observed during all three ignition cycles (last two columns in Table 2). In the absence of NO and in the presence of C₃H₆ the deactivation phenomenon as described in Fig. 1 can be observed, although all light-off curves are shifted to lower temperatures due to the absence of NO inhibition.

The results of Table 2 strongly suggest that the deactivation effect studied in this paper is due to the presence of C₃H₆. However, other reversible deactivation mechanisms are also known, such as the reversible oxidation of the precious metal by NO₂ [5] or oxygen

Table 1
Reaction and catalyst pretreatment conditions applied in this paper.

Process	SV/1000 h ⁻¹	Heating ramp K/min	Cooling ramp K/min	Holding time/min	c(CO)/ppm	c(C ₃ H ₆)/ppm	c(NO)/ppm	c(O ₂)/%	c(CO ₂)/%	c(H ₂ O)/%
Standard-IE-Exp	30	+10	-10	-	250	100	50	10	10	10
SV _{high} -IE-Exp	90	+10	-10	-	250	100	50	10	10	10
CO _{high} -IE-Exp	30	+10	-10	-	500	100	50	10	10	10
SV _{high} -CO _{low} -IE-Exp	90	+10	-10	-	50	100	50	10	10	10
oxidativeRe-conditioning (Reactivation)	equal to experiment	+10	-10	Various	-	-	-	10	10	10
N ₂ only Re-conditioning (Reactivation)	equal to experiment	+10	-10	Various	-	-	-	0	0	0

Table 2

Required temperature for 50 % CO conversion during the ignition branches of three consecutive ignition/extinction cycles performed in accordance to the standard ramping protocol shown in Fig. 1a). The experiments were performed once without NO, once without C₃H₆ and once without either NO or C₃H₆.

Ignition	Standard T _{50%} /°C	Without NO T _{50%} /°C	Without C ₃ H ₆ T _{50%} /°C	Without C ₃ H ₆ , NO T _{50%} /°C
1st	130	125	126.5	115
2nd	140	129.5	127.5	115.5
3rd	140	129	127	-

[7,9]. Since in general these effects have been observed at higher temperatures and after a reductive pretreatment, it is less likely that they contribute in a significant amount to the deactivation phenomenon discussed in this paper.

3.3. Reactivation of the catalyst

In our interpretation of the standard experiment it was implicitly assumed that any deactivation has been completely removed by the first lean conditioning ramp up to 400 °C in the absence of hydrocarbons. The idea would be that any hydrocarbon residues deposited at lower temperature would be burned-off at higher temperatures in the oxidizing atmosphere. In the following, we study the catalyst regeneration in a more systematic way.

To examine the reactivation behavior of the catalyst, a sequence of ignition extinction experiments was performed where the catalyst was reconditioned at different temperatures between 160 °C and 75 °C and the resulting activation state was probed by a subsequent ignition-extinction experiment. The ramping protocol is shown in Fig. 2a). Each experiment started with the pulse sequence of the standard experiment of Fig. 1 (oxidative conditioning at 400 °C followed by two ignition extinction experiments). Following this step, the catalyst was again conditioned in an oxidative atmosphere at a lower temperature (in this case 160 °C) and two further ignition extinction experiments were conducted. Fig. 2b) compares the first and the second CO light-off curve measured after the regeneration at 400 °C with the third and fourth CO light-off curves which were measured directly after the conditioning at 160 °C. The corresponding ignition curves for C₃H₆ are shown in the Supplementary material (Fig. S3).

It can be observed that the ignition curves obtained immediately after the two different conditioning phases (i.e. ignition 1 and 3) are essentially identical. From this observation we can conclude that the reactivation at 160 °C results in the same fully activated state as the reactivation at 400 °C. The subsequent ignition curves (2 and 4) require approximately 11 °C higher temperatures for 50 % CO conversion. It is evident that the intermediates are formed during or after the first C₃H₆ ignition. These intermediates block active sites on the catalyst's surface and lower its activity during the following ignitions. They can be completely removed by a temperature ramp up to 160 °C in the absence of pollutants.

Data for different conditioning temperatures are summarized in Table 3. The table reports the ignition temperature for 50 % CO conversion after the reactivation (3rd ignition). An ignition temperature of 130 °C corresponds to a complete recovery of the state obtained after the initial activation at 400 °C, while an ignition temperature of 140 °C corresponds to no reactivation, representing the same deactivated catalyst state as for the second (deactivated) ignition. (The required temperatures to reach 50% C₃H₆ ignition are provided as Supplementary material, see Table S1).

A temperature ramp up to 110 °C in an oxidative environment without pollutants is sufficient to reactivate the catalyst completely. Conditioning periods at temperatures from 75 to 100 °C still lead to a partial reactivation of the catalyst. At 75 °C no difference is found between conditioning times of 1000 s and 3600 s.

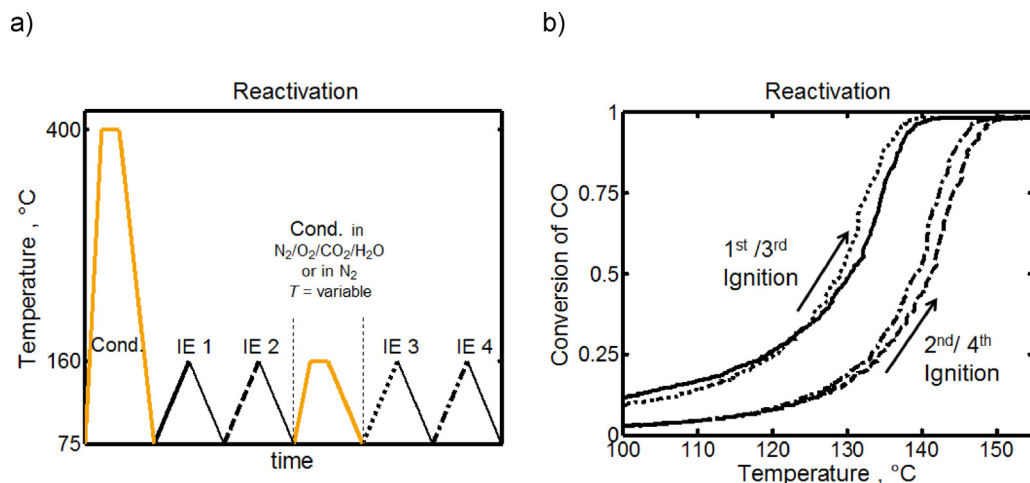


Fig. 2. After a conditioning in an oxidative environment at 400 °C two consecutive ignition extinction experiments were performed under standard conditions to deactivate the catalyst. Following this the catalyst was again conditioned at 160 °C to reactivate the catalyst before two more ignition extinction experiments were carried out. A schematic temperature ramp for the experiment is shown in a). The ignition curves for CO can be seen in b).

Table 3

Efficiency of the regeneration at different temperatures. Experiments were conducted as shown in Fig. 4a). The table reports the light-off temperature (50% CO conversion) of the third ignition (reactivated) as a function of the temperature and duration of the conditioning pulse. For reference, 130 °C was required during the first ignition (totally activated), while 140 °C was required during the second ignition (deactivated).

Conditioning	Oxidative T/°C	N ₂ only T/°C
160 °C, 300 s	130	130
140 °C, 3600 s	130	131
130 °C, 200 s	–	135
130 °C, 3600 s	–	135
120 °C, 3600 s	131	140
110 °C, 3600 s	131	–
100 °C, 3600 s	133	–
75 °C, 3600 s	133	140
75 °C, 1000 s	133	140

In addition to the experiments with an oxidative conditioning, a second series of experiments was conducted with a conditioning in N₂ only. The results of this series are also reported in Table 3. In contrast to the oxidative environment, a temperature ramp up to 140 °C is required to reactivate the catalyst completely in N₂. At 130 °C only a partial reactivation is achieved independent of the applied timescale while at 120 °C no reactivation occurs at all in N₂.

The fact that reactivation can occur in an oxidative environment in the absence of pollutants at temperatures of 75 °C while at least 130 °C are required to see a reactivation in N₂ is a strong evidence for at least two different reactivation mechanisms occurring on the catalyst surface.

3.4. The activation state above light-off temperature

At temperatures above the light-off, the ignition front will move continuously to the catalyst inlet as the feed temperature rises. Thus most of the catalyst is subjected to an HC-free gas mixture that is very similar in composition to the gas mixture applied during catalyst regeneration experiments discussed in Section 3.3. It can therefore be assumed that at high temperatures most of the catalyst is free of HC residues.

To verify this assumption the standard ignition-extinction experiment of Fig. 1 was repeated with different gas compositions during the heat-up so that each experiment provides a different catalyst history for the extinction. First, the catalyst was heated in

Table 4

Temperatures where 25, 50 and 75 % CO conversion occurs during the cool down branch for catalysts with different history before cool down: 1.: heating up in an oxidative environment (10% O₂, 10% H₂O, 10% CO₂, balance N₂) without pollutants, 2.: a standard ignition branch as in Fig. 1. 3.: a standard ignition branch followed by a 2500 s time period at 155 °C in the reaction gas mixture.

Measurement	T _{25%} /°C	T _{50%} /°C	T _{75%} /°C
After heat-up in 10% O ₂ , 10% H ₂ O, 10% CO ₂	118	125	128.5
After heat-up in reaction mixture	119	127	130
After heat-up in reaction mixture and 2500 s holding time	117	124	127.5

an oxidative environment (10% O₂, 10% H₂O, 10% CO₂, balance N₂) without pollutants above T_{100%} HC ignition temperature (155 °C) and then cooled in the pollutant containing standard gas mixture. Second, an ignition extinction experiment was performed with the pollutant containing feed mixture of the standard experiment. Finally, an ignition extinction experiment was carried out with the same standard pollutant containing gas mixture, holding the temperature at 155 °C for 2500 s. The extinction temperatures for 25, 50 and 75% CO conversion can be seen in Table 4. The corresponding data for the C₃H₆ conversion is provided as Supplementary material (see Table S2).

No significant differences between the extinction temperatures are observable for the different pretreatments. If HC intermediates remained stable on the surface after 100 % C₃H₆ conversion was reached, differences between the three extinction curves would be expected. Thus we can conclude that the catalyst is always in the same condition before the extinction branch starts. This observation can be regarded as strong evidence for a complete removal of HC residuals above 155 °C temperature.

3.5. Influence of space velocity and CO concentration on the deactivation effect

When investigating the deactivation behavior more systematically, we found that surprisingly the deactivation effect shown in Fig. 1 is not observed under all operating conditions. For example, the deactivation effect disappears if the experiments are performed at a higher space velocity or with a higher CO inlet concentration. Results of such experiments are reported in Table 5. All of the experiments provided in the table follow the procedure of the standard experiment of Fig. 1, except that the space velocity and the inlet CO concentrations were changed as indicated in the table. The corre-

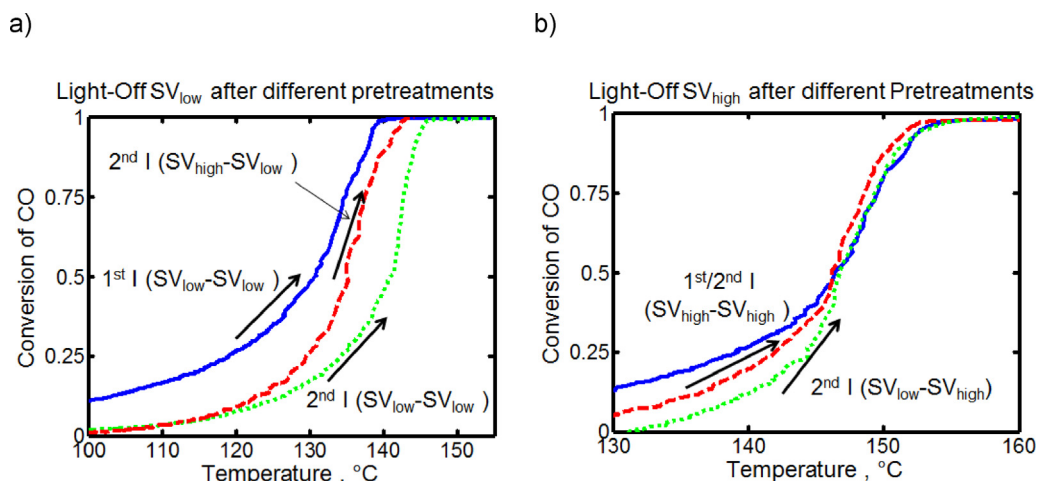


Fig. 3. Results of the cross-over experiments. a) Comparison of light of curves at low space velocity ($30,000 \text{ h}^{-1}$) with different pretreatment. Blue line: After activation, 1st ignition of standard experiment at low space velocity ($\text{SV}_{\text{low}}-\text{SV}_{\text{low}}$). Red dashed: After cool down at high space velocity, 2nd ignition of cross over experiment $\text{SV}_{\text{high}}-\text{SV}_{\text{low}}$. Green dotted: After cool down at low space velocity, 2nd ignition of standard experiment at low space velocity ($\text{SV}_{\text{low}}-\text{SV}_{\text{low}}$). b) Comparison of light of curves at high space velocity ($90,000 \text{ h}^{-1}$) with different pretreatment. Blue line: After activation, 1st ignition of standard experiment at high space velocity ($\text{SV}_{\text{high}}-\text{SV}_{\text{high}}$). Red dashed: After cool down at high space velocity, 2nd ignition of standard experiment at high space velocity, $\text{SV}_{\text{high}}-\text{SV}_{\text{high}}$. Green dotted: After cool down at low space velocity, 2nd ignition of the cross over experiment ($\text{SV}_{\text{low}}-\text{SV}_{\text{high}}$). (For interpretation of the references to colour in this figure legend, the reader is referred to the web version of this article.)

Table 5

The influence of space velocity and CO concentration on the deactivation effect. The table reports the required temperature for 50% CO conversion during the first and the second ignition. All experiments follow the procedure of Fig. 1 with only the space velocity and the CO concentration changed as indicated in the following. SV high: $\text{SV} = 90,000 \text{ h}^{-1}$ (standard = $30,000 \text{ h}^{-1}$), CO high: $\text{Xco} = 500 \text{ ppm}$ (standard (250 ppm), CO low: $\text{Xco} = 50 \text{ ppm}$ (standard (250 ppm)).

CO	Standard	SV high	CO high	SV high, CO low
1st Ignition $T_{50\%}/^{\circ}\text{C}$	130	146	151.5	109
2nd Ignition $T_{50\%}/^{\circ}\text{C}$	140	146	153	118
$\Delta T/^{\circ}\text{C}$	10	0	1.5	9

sponding light-off temperatures for C_3H_6 as well as the full light-off curves are presented in the accompanying material Table S3, Figs. S4–S6, respectively.

It is observed that the deactivation effect completely disappears if the space velocity is increased from $30,000 \text{ h}^{-1}$ to $90,000 \text{ h}^{-1}$. If the CO concentration is increased from 250 ppm to 500 ppm, the deactivation effect also nearly disappears. It is noticeable that in both experiments where the deactivation phenomenon disappears the light-off temperature is increased compared to the standard experiment (due to increased CO inhibition or due to decreased residence time). It is therefore an obvious assumption that the deactivation effect might be linked to the light-off temperature, possibly because the proposed hydrocarbon residues are less stable at higher temperatures.

To test this assumption further, an experiment was carried out at the high space velocity ($90,000 \text{ h}^{-1}$) but at very low CO concentration (50 ppm) so that the effect of space velocity on the light-off temperature was offset by reduced CO inhibition. This experiment had a lower light-off temperature than the standard experiments and in agreement with our assumption, the deactivation effect was observed again.

3.6. Cross-over experiments, first and second cycle at different space velocities

There are two possible explanations for the fact that the difference between first and second light-off disappears at higher space velocities or CO concentrations:

1. The hydrocarbon residues are not stable at the higher extinction temperatures and hence less residue is formed at higher extinction temperatures. Thus, no HC intermediates would be formed under these reaction conditions and no deactivation phenomenon would be observed.
2. Under conditions with an increased light-off temperature, the formation of HC intermediates during the ignition branch might be sufficient, so that the initial state (the HC residuals deposited during the cool-down) would not play a crucial role anymore. Possible reasons for the increased deposition during the ignition might be higher deposition rates at the higher light-off temperature or simply the increased time until light off is reached.

To distinguish between these two possible scenarios more clearly, the standard experiment of Fig. 1 was repeated using different space velocities in the first and the second ignition extinction cycle. In the following we denote an experiment where the first cycle is conducted at a high space velocity ($90,000 \text{ h}^{-1}$) and second cycle at a lower space velocity ($30,000 \text{ h}^{-1}$) as $\text{SV}_{\text{high}}-\text{SV}_{\text{low}}$. The experiment which used a low space velocity in the first cycle and a high velocity in the second cycle is denoted $\text{SV}_{\text{low}}-\text{SV}_{\text{high}}$.

First we discuss results for the cross over experiment with the high space velocity ($\text{SV}_{\text{high}}-\text{SV}_{\text{low}}$). Fig. 3a) shows the light of curve for the second ignition, which was performed at a low space velocity. These data are compared to the two ignition curves obtained during the standard experiment at the same low space velocity. It is observed that the ignition curve after the cool-down at the higher space velocity lies between the lightoff curves for the activated catalyst and that obtained after the cool down at the lower space velocity. From these results one can conclude, that during the cool-down at the higher space velocity (and hence higher extinction temperature) some HC intermediates are deposited on the catalyst surface, although in smaller amounts than during the extinction branch of the low SV experiment.

Results for the $\text{SV}_{\text{low}}-\text{SV}_{\text{high}}$ experiment are shown in Fig. 3b). This figure shows the light-off curve for the second ignition (performed at high space velocity) which is compared to the first and second ignition curve of a standard experiment performed at the same high space velocity. The initial activities are in line with our conclusion from Fig. 3a: The highest activity is observed for the

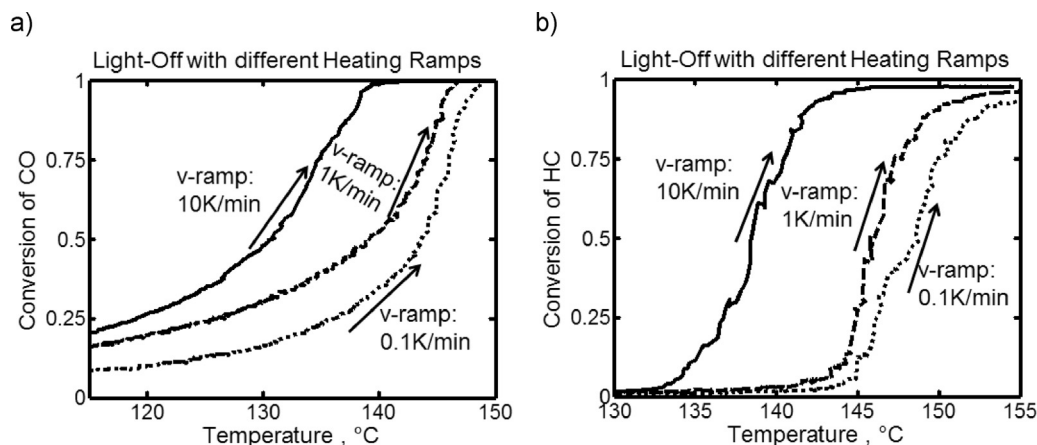


Fig. 4. comparison of three (a) CO and (b) C₃H₆ ignition curves recorded with different heating ramps (10 K/min, 1 K/min and 0.1 K/min) in the standard gas mixture, each after a conditioning in an oxidative environment to show the impact of the heating rate on the catalyst's deactivation. Accept of the heating rate all experiments were performed under standard conditions (see Table 1).

catalyst after regeneration, the lowest activity for the cross over experiment where the catalyst was cooled down at low space velocity. The activity of the catalyst cooled down at high SV is between the other two curves. However, as the temperature increases, the differences become smaller and by the time when 50% CO conversion is reached, the activity is independent of the pretreatment. These results support the second of the two possible explanations proposed above, i.e. that at the higher light-off temperatures the formation of the deposits is so fast that the initial deposits from the previous cool-down become irrelevant.

3.7. Influence of the heating ramp

In this section, the influence of different heating ramps on the CO and C₃H₆ ignition curves is investigated.

For this investigation three experiments with different heating ramps were performed. For each experiment, a conditioning in an oxidative environment was applied to the catalyst, followed by a subsequent ignition experiment, once with a heating ramp of 10 K/min, once with a heating ramp of 1 K/min and once with a heating ramp of 0.1 K/min. The ignition curves plotted vs. the temperature can be seen in Fig. 4a) for CO and in Fig. 4b) for C₃H₆.

While approximately 132 °C are sufficient to achieve 50% CO conversion with a heating ramp of 10 K/min, 139 °C and 143 °C are required with temperature ramps of 1 K/min and 0.1 K/min respectively. The C₃H₆ ignition curves shift to 7 and 9 °C higher temperature with decreasing heating rates. Thus the ignition curves obviously shift to higher temperatures with decreasing heating rates.

It is well known that, due to the thermal inertia of the catalyst, light-off curves (plotted versus the inlet temperature) shift to higher temperatures as the ramp rate is increased [20]. However, note that the trend observed in our experiments is the opposite of what is expected due to thermal inertia, so that our results cannot be explained by thermal effects. We believe that the increase in the light-off temperatures shown in Fig. 4 has not been discussed in the literature before and can be explained by the deactivation due to HC species on the catalyst surface. Due to the oxidative conditioning, it can be assumed that at the beginning of all three light-off tests, the catalyst is free of HC residuals. As the catalyst is heated and conversion starts, hydrocarbon residuals are formed. With slow heating rates, there is more time until a given temperature is reached and hence more residuals can build up, shifting the ignition curve to higher temperatures.

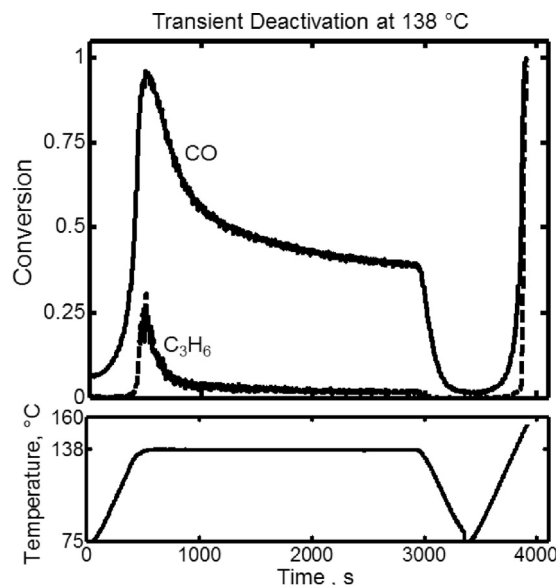


Fig. 5. Deactivation experiments at a constant temperature to show the dynamic deactivation effect over time and to achieve the highest degree of catalyst deactivation for the applied reaction conditions. The figure shows the catalyst inlet temperature profiles as well as the CO and C₃H₆ conversion during the deactivation periods of 2500 s at a constant temperature of 138 °C, followed by a subsequent ignition experiment. The experiment was performed under standard conditions after an oxidative pretreatment at 400 °C.

3.8. Transient deactivation at constant temperature

Finally, we present two experiments that allow the direct observation of the transient deactivation in the time domain with the catalyst kept at a fixed temperature. The first experiment initially follows the standard procedure of Fig. 1 (oxidative regeneration followed by a heating ramp). During the first heat-up in the reaction mixture, the ramp was stopped at a temperature of 138 °C (where little HC ignition occurs). The temperature was then kept constant for 2500 s before the catalyst was cooled again and a second standard ignition-extinction cycle was performed. Fig. 5 shows the CO and HC conversion during the first heat up and the subsequent constant temperature phase. It was found that as soon as the temperature ramp was stopped, the CO and the HC conversion started to drop before a steady state conversion was reached after ~ 2300 s. The observed drop in the catalyst activity can be attributed to the

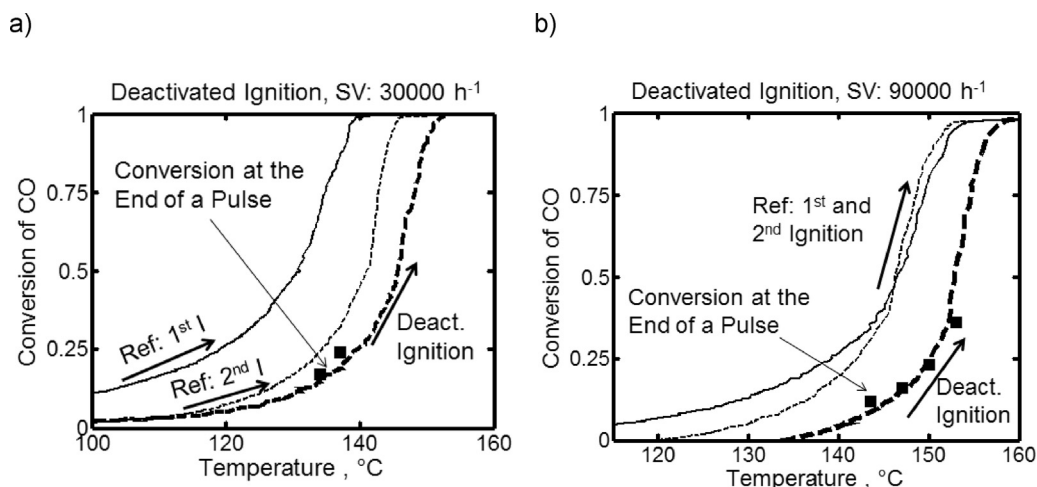


Fig. 6. Comparison between the ignition curves obtained after the deactivation period of Fig. 5 (completely deactivated) with the amount of conversion at the end of the deactivation pulses (see Fig. 7) as well as with the ignition curves recorded during two consecutive ignition extinction cycles are depicted in a) for a SV of 30,000 h⁻¹ and b) for a SV of 90,000 h⁻¹.

progressive deactivation of the catalyst so that the experiment provides an idea about the timescale of the deactivation process.

Fig. 6 plots the CO conversion during the second heat-up following the 2500 s at constant temperature and subsequent cool-down for the experiment of Fig. 5. As a reference, the plot also shows the first and second light-off curve of the standard experiment of Fig. 1. Obviously, the extended time at 138 °C leads to an additional deactivation compared to the deactivation obtained after the standard ignition-extinction cycle. The experiment of Fig. 5 was repeated with different plateau temperatures and it was found that temperatures in the range of 130 °C–142 °C yielded identical deactivation levels (see Fig. S10 in the Supplementary material). Holding the temperature at 100 °C only led to a partial deactivation. The experiment of Fig. 5 was also repeated at the higher space velocity of 90,000 h⁻¹ (see Supplementary material Fig. S8). In this case the holding temperature was chosen as 148 °C. It is interesting to note that also in this case holding the catalyst near the light-off temperature for 2500 s leads to an additional deactivation compared to the deactivation during the standard ignition-extinction cycle. This result seems somewhat unexpected since in section 6 (cross-over-experiments) we have shown that at the high space velocity the 50% light-off temperature is insensitive to the initial deactivation level, which was explained by a fast deposition of hydrocarbon residues during the heat-up making the initial hydrocarbon residues irrelevant. Obviously this is only true for the moderate deactivation levels achieved during the standard ignition-extinction cycle.

To provide a direct measurement of the deactivation kinetics at different temperatures, a second type of transient experiment was performed (see Fig. 7). In this experiment, the catalyst was heated to a target temperature in an oxidative environment without pollutants. Then, the standard gas mixture was applied to the catalyst for 2500 s and the deactivation was studied by following the CO and HC conversion. Following this, the catalyst was regenerated in an oxidative environment and at the same time heated to a new target temperature (approximately 3 °C higher than previous temperature), before the standard gas mixture was again applied. This procedure was conducted at space velocities of 30,000 h⁻¹ and 90,000 h⁻¹. The results are shown in Fig. 7a) and b), respectively. At all temperatures a transient deactivation can be observed. Generally, a stationary state is reached faster at the higher space velocity. While a stationary state in CO and C₃H₆ conversion is reached for all investigated temperatures at a space velocity of 90,000 h⁻¹, it is only obtained for 135 and 138 °C at a space velocity of 30,000

h⁻¹. For those conditions where a stationary CO conversion was reached, the steady state conversions measured at the end of the 2500 s are included in Fig. 6. The points all fall on the ignition curves recorded after the deactivation period of Fig. 6, a further confirmation of our earlier conclusion that independent of the deactivation temperature, after a long deactivation time the same steady state deactivation level is obtained, as long as the temperature during the deactivation is above a certain threshold.

3.9. Summary of the qualitative discussion

In the previous sections, along with the presentation of the experimental results, we have provided a qualitative discussion of the observed phenomena and we have shown that the observations can qualitatively be explained by the reversible site blocking due to hydrocarbon residuals. This qualitative discussion was based on a limited number of assumptions about the nature and behavior of the site blocking species. Table 6 summarizes this previous discussion, i.e. it lists the assumptions made throughout the preceding discussion together with experimental evidence supporting each of the assumptions. The summary of Table 6 will form the basis for the construction of a kinetic model and a more quantitative discussion that is presented in the following section.

3.10. Simulation based quantitative discussion

3.10.1. Model description

As an aid in elucidating and discussing the role of the HC intermediates, we have cast the assumptions of Table 6 into a kinetic model. The resulting reactions are listed in Table 7, the kinetic parameters are provided in Tables S4 and S5 of the Supplementary material.

It was found that the experimentally observed deactivation behavior can be well represented by a simple model that assumes that HC residuals can only cover a certain fraction of the platinum surface. A simple way to implement this behavior is to assume two different platinum sites A₁ and A₂, where HC residuals only adsorb on sites A₂.

Reactions 1–2 represent CO and HC oxidation on site A₁, reactions 3–4 the same reactions on site A₂. Reaction 5 describes the formation of partial oxidation products on site A₂, which in this paper are denoted collectively as HCO, without further specification of the individual species. Reaction 6 describes the oxidation of

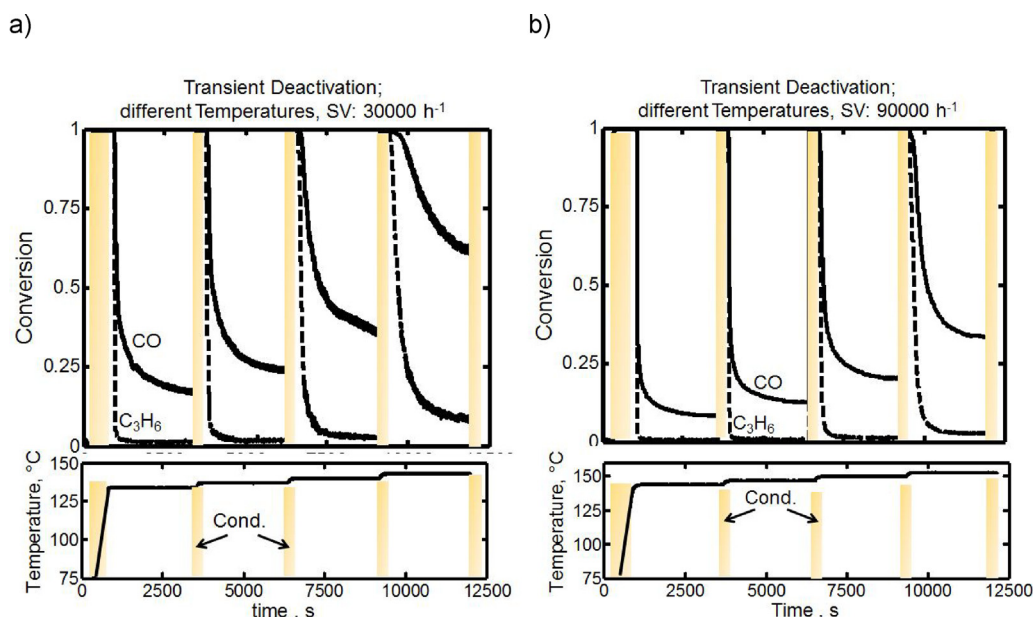


Fig. 7. Deactivation experiments at different temperatures on the HC ignition curve to investigate the deactivation behavior at different degrees of conversion. The temperature ramps as well as the CO and C₃H₆ conversion during the 2500 s long deactivation pulses preceded by a heating sequence in an oxidative environment without pollutants are depicted in a) for a SV of 30,000 h⁻¹ and b) for a SV of 90,000 h⁻¹. The procedure was preceded by an oxidative conditioning at 400 °C. The applied pollutants concentration corresponded to the standard values of Table 1.

Table 6

Summary of the assumptions about the HC induced deactivation phenomenon and the supporting evidence underpinning each assumption.

Assumption	Supporting Evidence
The reversible deactivation is due to hydrocarbon residuals that consist of partial oxidation products which are deposited at those locations where the HC conversion takes place.	DRIFTS-detection by Abedi et al. [16] and results of Table 2 (no deactivation during consecutive ignition extinction experiments without C ₃ H ₆).
At low temperatures, where no HC conversion occurs, the surface coverage by HC intermediates remains constant.	Supplementary material: Fig. S10 (at low temperatures around 100 °C the deactivation progress is very slow. As a logical consequence it can be expected that at even lower temperatures no further formation of HC intermediates occurs) and Table 3 (at temperatures lower than 130 °C no reactivation occurs in N ₂ only. Thus a removal of the intermediates in a constant gas mixture containing pollutants is unlikely).
At high temperatures well above the ignition temperature the residuals are removed by total oxidation.	Results of Table 4 (no differences in the extinction branch after different catalyst pretreatments).
In addition to occurring in an oxidative environment, reactivation also occurs in an oxygen free atmosphere.	Results of Table 3 (conditioning in N ₂ leads to a total reactivation at 140 °C).
The residuals can be formed during the ignition and the extinction branch of a heating and cooling cycle.	<i>Ignition branch:</i> Results of Fig. 4 (slower heating ramps lead to higher ignition temperatures) and Fig. 5 (transient deactivation: a decline in conversion is observed at constant temperature on the HC ignition curve). <i>Extinction branch:</i> Standard experiment (Fig. 1) Delayed ignition during second and third light-off.
At high ignition/extinction temperatures the total oxidation of C ₃ H ₆ occurs faster than the partial oxidation. Therefore fewer intermediates are formed on the catalyst surface under conditions with higher light-off temperatures, i.e. at higher space velocities and pollutants concentrations.	Results of Table 5 (comparison of consecutive ignition curves at higher SVs and CO concentrations doesn't show a difference above 50 % conversion) and Fig. 3 (cross-over-experiments: the ignition curve recorded at the higher space velocity is insensitive to the preceding extinction experiment)
After a long deactivation (>2500 s) the same deactivation state is obtained independent of the at which temperature the deactivation was performed.	Results of Section 3.7.

the partial oxidation products HCO to CO₂. Since in Table 6 it was observed that also a heating ramp in nitrogen leads to a catalyst regeneration, the thermal desorption of partial oxidation products was added as reaction 7. Due to reaction 7, the model predicts the emission of HCO. Since the overall amount of HCO stored on the catalyst is low, we did not check experimentally for the emission of any partial oxidation products.

Please note that we do not claim that these reactions are fundamentally correct. It is quite possible, indeed rather likely that other reaction combinations which mirror the assumptions of Table 6 can be fitted to the experimental data.

The main purpose of the model, and this section, is to show that it is possible to capture the activation/deactivation features with rel-

atively few assumptions, and to use the model to offer some insight into the experimental results and to illustrate the phenomenon.

The reactor model used is described in Hauptmann et al. [19]. The rate equations for the seven reactions are also listed in Table 7.

The preexponential factors and the activation energies for the 7 reactions (14 free parameters in total) were determined by fitting the model to the experiments shown in Figs. 1, 3, 4 and 5 (Standard Experiment, Cross-Over-Experiment, Ignition with different heating ramps and Transient Deactivation). It is worthwhile to note that we do not propose that the parameters thus found are necessarily the only combination of parameters that will give an acceptable fit to the data. Rather, as noted above, our purpose is to use the model to help us to interpret and discuss the results.

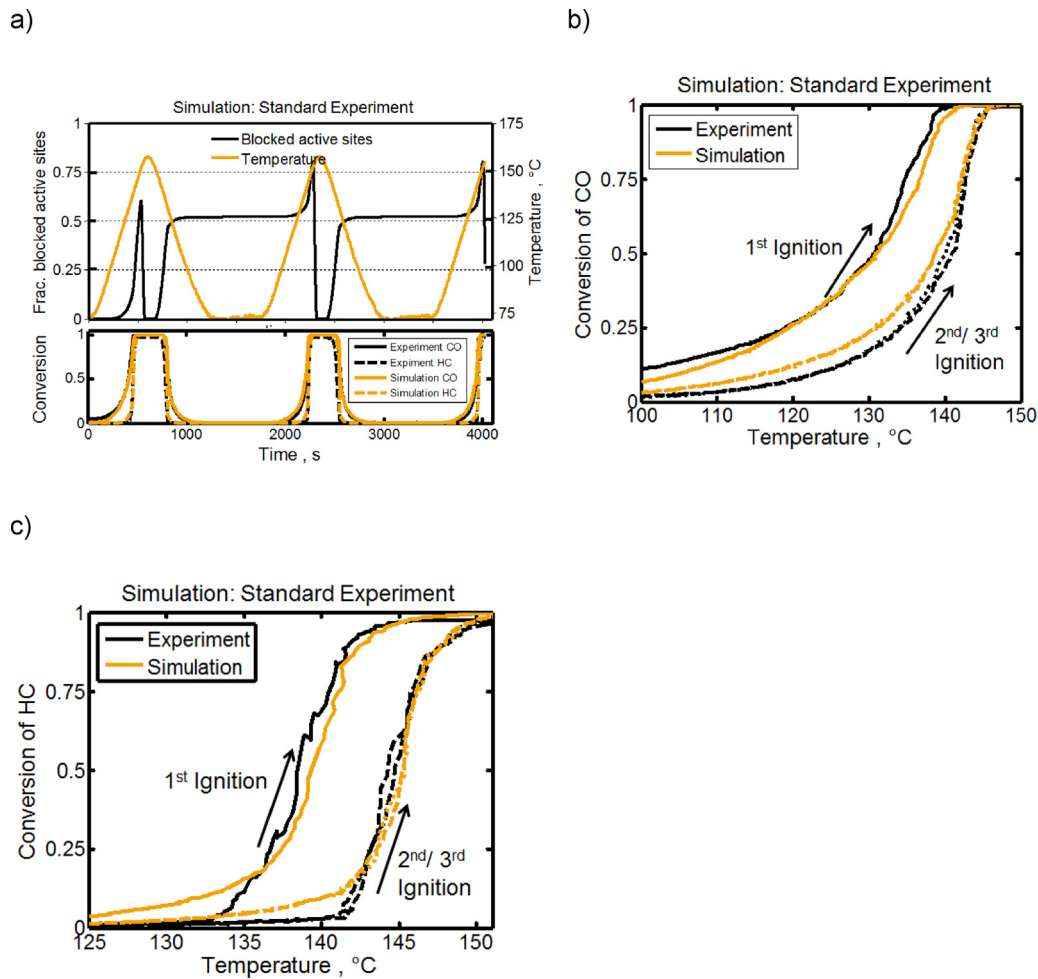


Fig. 8. Simulation of the standard experiment of Fig. 1a) Temperature ramp for three subsequent ignition extinction experiments and the simulated fraction of blocked active sites A_2^* (average value over axial catalyst channel). A comparison between the experimental and the simulated ignition curves are depicted in b) for CO and in c) for C₃H₆.

Table 7

Reactions incorporated in the kinetic model and the corresponding rate equations. r_i is the rate of reaction i , k_i is the corresponding rate constant, y_j is the concentration of species j . The rate equations for the reactions involving gas species include an inhibition term G_1 based on Oh and Cavendish [21]: $G_1 = T \cdot (1 + K_1 \cdot y_{CO} + K_2 \cdot y_{C_3H_6})^2 \cdot (1 + K_3 \cdot (y_{CO} \cdot y_{C_3H_6})^2) \cdot (1 + K_4 \cdot y_{NO})$. The rate constants k and the sorption constants K for the surface reactions and inhibition are calculated using the classical Arrhenius temperature dependence. The parameters for the inhibition term are adopted from Herrmann [22], so that the model contains 14 free parameters that have been fit to the data (one pre-exponential factor and one activation energy for each reaction). The fitted parameters are listed in Tables S4 and S5 of the supplementary material.

Oxidation of CO, HC on site 1		
R1	$CO + 0.5 O_2 + A_1^* \rightleftharpoons CO_2 + A_1^*$	$r_1 = k_1 \cdot y_{A_1^*} \cdot y_{CO} \cdot y_{O_2} / G_1$
R2	$C_3H_6 + 4.5 O_2 + A_1^* \rightleftharpoons 3 CO_2 + 3 H_2O + A_1^*$	$r_2 = k_2 \cdot y_{A_1^*} \cdot y_{C_3H_6} \cdot y_{O_2} / G_1$
Oxidation of CO, HC on site 2		
R3	$CO + 0.5 O_2 + A_2^* \rightleftharpoons CO_2 + A_2^*$	$r_3 = k_3 \cdot y_{A_2^*} \cdot y_{CO} \cdot y_{O_2} / G_1$
R4	$C_3H_6 + 4.5 O_2 + A_2^* \rightleftharpoons 3 CO_2 + 3 H_2O + A_2^*$	$r_4 = k_4 \cdot y_{A_2^*} \cdot y_{C_3H_6} \cdot y_{O_2} / G_1$
Deactivation of site 2		
R5	$C_3H_6 + 1 O_2 + A_2^* \rightleftharpoons A_2^* - HCO$	$r_5 = k_5 \cdot y_{A_2^*} \cdot y_{C_3H_6} \cdot y_{O_2} / G_1$
Reactivation of site 2		
R6	$3.5 O_2 + A_2^* - HCO \rightleftharpoons A_2^* + 3 CO_2 + 3 H_2O$	$r_6 = k_6 \cdot y_{A_2^*} \cdot y_{A_2^* - HCO} \cdot y_{O_2} / G_1$
R7	$A_2^* - HCO \rightleftharpoons A_2^* + HCO$	$r_7 = k_7 \cdot y_{A_2^*} \cdot y_{A_2^* - HCO}$

3.10.2. Simulation of the standard experiment

The first simulation shown in Fig. 8 represents the experimental results from Fig. 1. The applied temperature ramp, the simulated fraction of active sites (A_2^*) blocked by the HC residuals (average

value over the channel) as well as the experimental and the simulated conversion of CO and C₃H₆ vs. time are provided in Fig. 8a). The three experimental and simulated consecutive ignition curves plotted vs. the temperature can be seen in Fig. 8b) for CO and in Fig. 8c) for C₃H₆.

It is seen from Fig. 8b) and c) that the experimental light-off curves are reproduced well in all cases, thus this model can describe the data well including the deactivation phenomenon. Fig. 8a) shows that the model suggests the formation of intermediates during ignition, so that at the time of light-off there is a significant site blocking already. As the temperature reaches the level corresponding to complete C₃H₆ conversion, the intermediates are all consumed, and no residuals remain on the surface. During the extinction branch, the HC residuals are formed again, leading to a roughly 50 % surface coverage when the extinction ramp is completed. Thus the second ignition curve starts from a state in which much of the surface is blocked, leading to a higher light-off temperature for the second ignition curve. This behavior is reproduced for the third ignition curve. The surface coverage predicted by the model is consistent with our hypotheses made from the experiment shown in Fig. 1, which can be summarized as:

- The concentration of adsorbed HC intermediates on the surface after 100% C₃H₆ conversion is negligible.
- HC intermediates can be formed during the ignition as well as during the extinction branch.

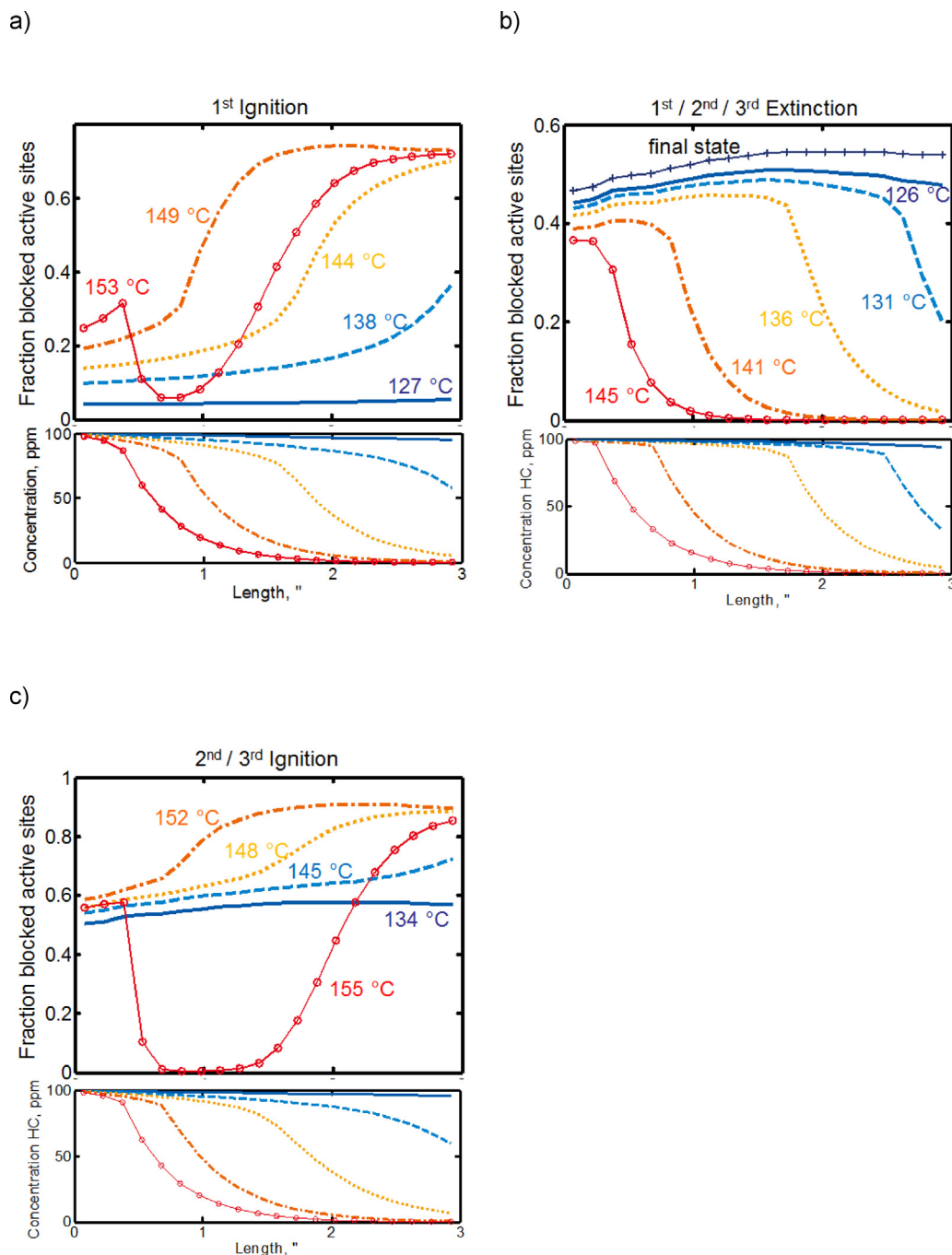


Fig. 9. simulated axial profiles of the fraction of HC blocked active sites A_2^* as well as the concentration of C_3H_6 in the gas phase at different states of a) the first ignition, b) the extinctions and c) the second/ third ignition of the standard experiment shown in Fig. 8.

– The HC intermediates formed during the extinction branch are responsible for the visible deactivation which causes the increase in the light-off temperature for the subsequent ignition curves, because they cause the difference of the catalyst initial state.

– At low temperature where no C_3H_6 conversion occurs, the surface coverage by HC intermediates is fixed.

We can gain insight into the reactor behavior by examining the axial concentration profiles predicted by the model. The axial profiles of the amount of C_3H_6 in the gas phase as well as the fraction of active sites A_2^* blocked by HC are given in Fig. 9a) for the first ignition curve, which corresponds to an initially clean surface. The axial profiles during the second ignition (initially surface partially filled) and the extinction branch can be seen in Fig. 9b) and c) respectively.

Consider the profiles of the adsorbed intermediates for the first ignition curve. Because we start with a clean surface, no intermediates are initially present. As the temperature increases and the reactor heats, HC deposits begin to form and an axial profile develops. While the overall C_3H_6 conversion remains below 100%, there will always be a gas phase concentration present, thus the concentration of adsorbed intermediates continuously rises, reaching a maximum at the reactor exit. At higher temperatures, the conversion reaches 100% before the end of the reactor, which implies that an HC free oxidizing atmosphere exists, and the concentration of blocking species begins to fall. Finally, at sufficiently high temperature, most of the reactor gas phase is HC free and the surface concentration is negligible. The profile of blocked active sites

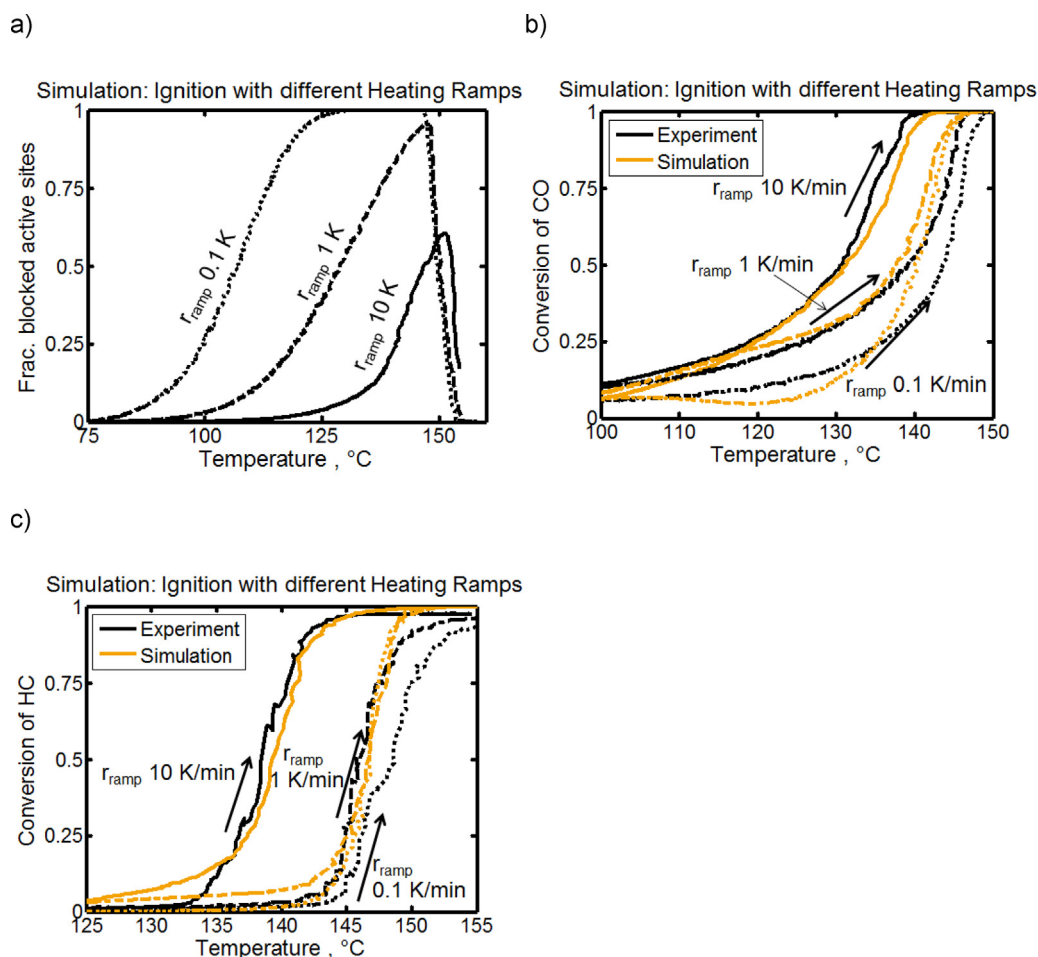


Fig. 10. Simulation of ignition curves with different heating ramps: a) Simulated fraction of blocked active sites A_2^* (average value over one channel) during three ignition experiments with different heating ramps (10 K/min, 1 K/min and 0.1 K/min) recorded in the standard gas mixture at a SV of $30,000 \text{ h}^{-1}$ always after a conditioning in an oxidative environment. A comparison between the simulated and the experimental conversion of CO and C_3H_6 can be seen in b) and c).

at 152°C shows a minimum in the first third of the reactor. This minimum can be explained by a temperature maximum due to the exothermic ignition process.

Considering the extinction curve, the initial condition shows that most of the surface is free of intermediates. However, as the reactor temperature falls at the reactor inlet, and the decreasing temperature wave progresses towards the reactor outlet, the adsorbed concentration builds at the inlet and a corresponding wave of adsorbed intermediates follows the temperature wave. Finally, as the temperature falls below that required to sustain a reaction, a steady state level of surface coverage results. The axial profiles of the adsorbed intermediates for the second ignition curve follow the same trend as the first one, albeit they start from a surface that has a significant coverage of adsorbed HC intermediates.

3.10.3. The effect of temperature ramp rates

We next consider the experiments performed at different temperature ramp rates (see Fig. 4). Fig. 10 compares the simulation results with the experimental data for the three ignition experiments. The simulated fraction of active sites (A_2^*) blocked by the HC residuals (cumulative value over the channel) is shown in Fig. 10a), whilst the three experimental and simulated ignition curves can be seen in Fig. 10b) and c) for CO and for C_3H_6 respectively.

As noted earlier, the trend in increasing light-off temperature with slower temperature ramps is opposite to what is expected if only thermal effects are considered. Assuming that lower ramping rates lead to an increased deposition of inhibiting intermediates

would provide a plausible explanation for experimentally observed higher light-off temperatures at slower ramp rates. Indeed, this pattern is suggested by the model, as shown in Fig. 10a). For a given reactor inlet temperature, more HC residuals are deposited on the catalyst surface during an ignition branch with a slow heating ramp compared to an ignition branch with a fast ramp. Thus, with an applied heating ramp of 0.1 K/min, the model indicates a complete blocking of active sites A_2^* at 125°C , while only a maximum blocking of 60% is predicted for a heating ramp of 10 K/min at 150°C (close to 100% C_3H_6 conversion). This enhanced blocking of active sites leads to a shift of the predicted light-off to higher temperatures, which is qualitatively in line with the experimental results. We observe that the fit of the light-off curves at the slower temperature ramps is not as good as for the fast one, however, the trend is correct and thus the inferences made should also have merit.

3.10.4. The cross-over experiment $SV_{\text{high}}-SV_{\text{low}}$

Next, we discuss the cross-over experiment where a first ignition/extinction cycle at high space velocity is followed by a second cycle at low space velocity, see Fig. 3.

Fig. 11 compares simulated results and experimental data of the standard experiment (Fig. 11a, both cycles at low space velocity) with the cross over experiment (Fig. 11b). The experimental and the simulated second CO ignition curve of the $SV_{\text{high}}-SV_{\text{low}}$ experiment plotted vs. the temperature can be seen in Fig. 11c). The first and the second ignition curve of the standard experiment ($SV_{\text{low}}-SV_{\text{low}}$) are provided as References

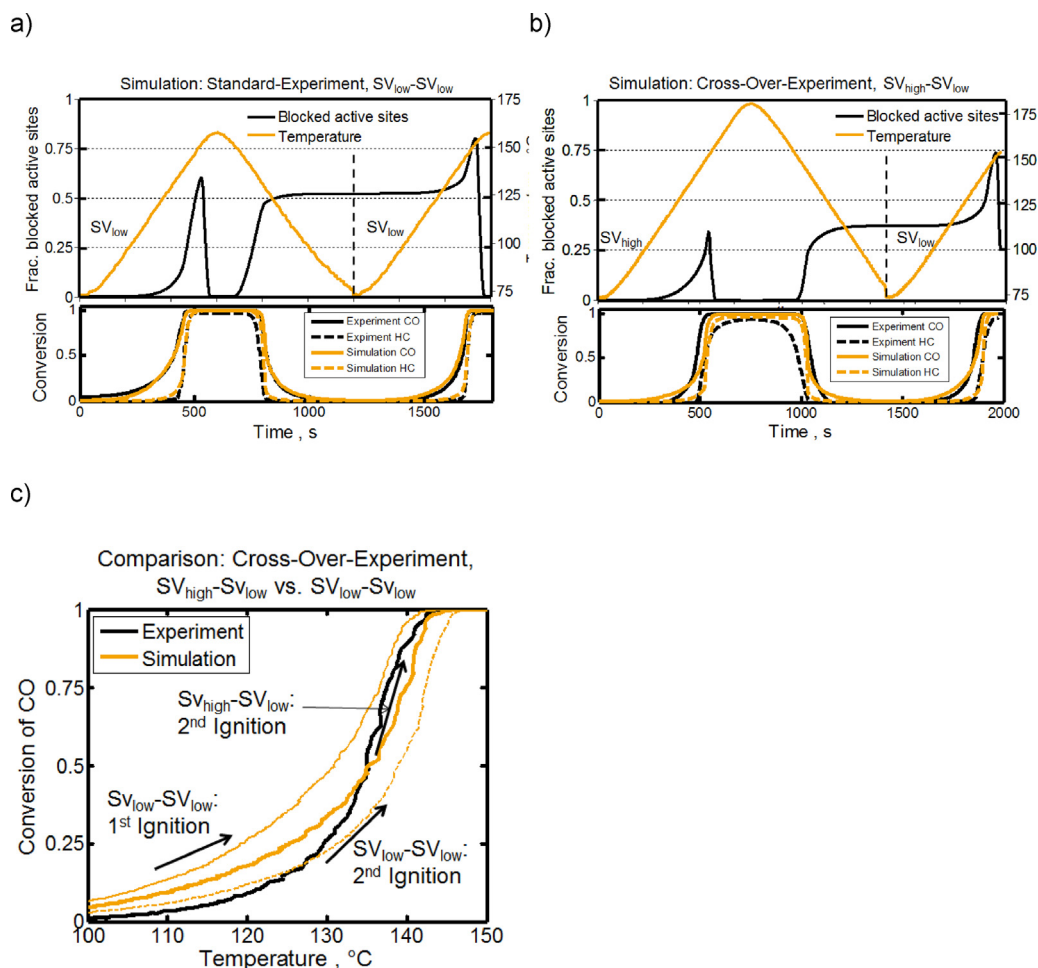


Fig. 11. Comparison of the cross-over experiment $SV_{high}-SV_{low}$ ($90,000\text{ h}^{-1}-30,000\text{ h}^{-1}$) with the standard experiment $SV_{low}-SV_{low}$: a) The temperature ramps and the simulated fraction of blocked active sites A_2^* (average value over axial catalyst channel) for the standard experiment $SV_{low}-SV_{low}$. Top: Temperature profile and computed fraction of blocked sites A_2^* . b) the corresponding data for the $SV_{high}-SV_{low}$ experiment. c) A comparison between the simulated results for first and second ignition of the standard experiment and the second ignition during the cross over experiment $SV_{high}-SV_{low}$. For reference, also the experimental data for the second ignition during the cross over experiment $SV_{high}-SV_{low}$ is shown.

Comparing Fig. 11a) and b) it is clear that during a high space velocity ignition experiment fewer surface intermediates are formed. The maximum total coverage is less during ignition, and the final value after extinction is also lower. Thus, when starting a new ignition experiment at low space velocity, the high-low combination starts with a lower initial surface coverage than the low-low case, and thus the second ignition curve will have a lower light-off temperature when it was preceded by an ignition-extinction experiment conduction at high space velocity. Fig. 11c) also shows that in the simulation the catalyst cooled down at the high space velocity shows a light-off activity between the fully activated catalyst and the catalyst cooled down at the lower space velocity. This is in good agreement with the experimental results of Fig. 3a.

3.10.5. Transient deactivation at constant inlet conditions

Finally, we compare the experimental and simulated results for the transient deactivation runs. Consider the result of Fig. 5, where the temperature was increased to 138°C in a standard ignition ramp, and then held there for 2500 s before the extinction curve was performed. This sequence was followed by a further ignition curve, which had a higher light-off temperature than the case without the extended holding time. We also recall that during the 2500 s hold at 138°C , the conversion of CO continued to fall, which would imply a buildup of HC intermediates on the surface. Fig. 12 compares the simulation results with the experimental data of the transient deac-

tivation experiment at 138°C . The applied temperature ramp, the simulated fraction of active sites (A_2^*) blocked by the HC residuals (average value over the channel) as well as the experimental and the simulated conversion of CO and C_3H_6 vs. time is shown in Fig. 12a). The experimental and simulated consecutive ignition curve plotted vs. the temperature can be seen in Fig. 12b) for CO and in Fig. 12c) for C_3H_6 . The simulated first and the second ignition curve of the standard experiment are added as References

As expected, the model does indeed show an increase in adsorbed intermediates during the holding time at 138°C . The concomitant decline in the CO conversion is also well tracked, as are the subsequent light-off curves for CO and HC.

The transient deactivation experiment shows a different behavior when the ignition ramp is only allowed to proceed to 100°C and then held for a 2500 s long deactivation. Fig. 13 compares the simulations with the experimental data of the transient deactivation experiment at 100°C .

In accordance with the expectations, the simulation predicts a slow accumulation rate of HC intermediates on the catalyst surface, which results only in an active site (A_2^*) blocking of approximately 15 % at 100°C . This value is smaller than the predicted blocking for an ignition/extinction cycle of the standard experiment (approximately 50 % see Fig. 8). Consequently, the subsequent ignition curve recorded after the deactivation period should lie between the first and the second ignition curve of the standard experiment.

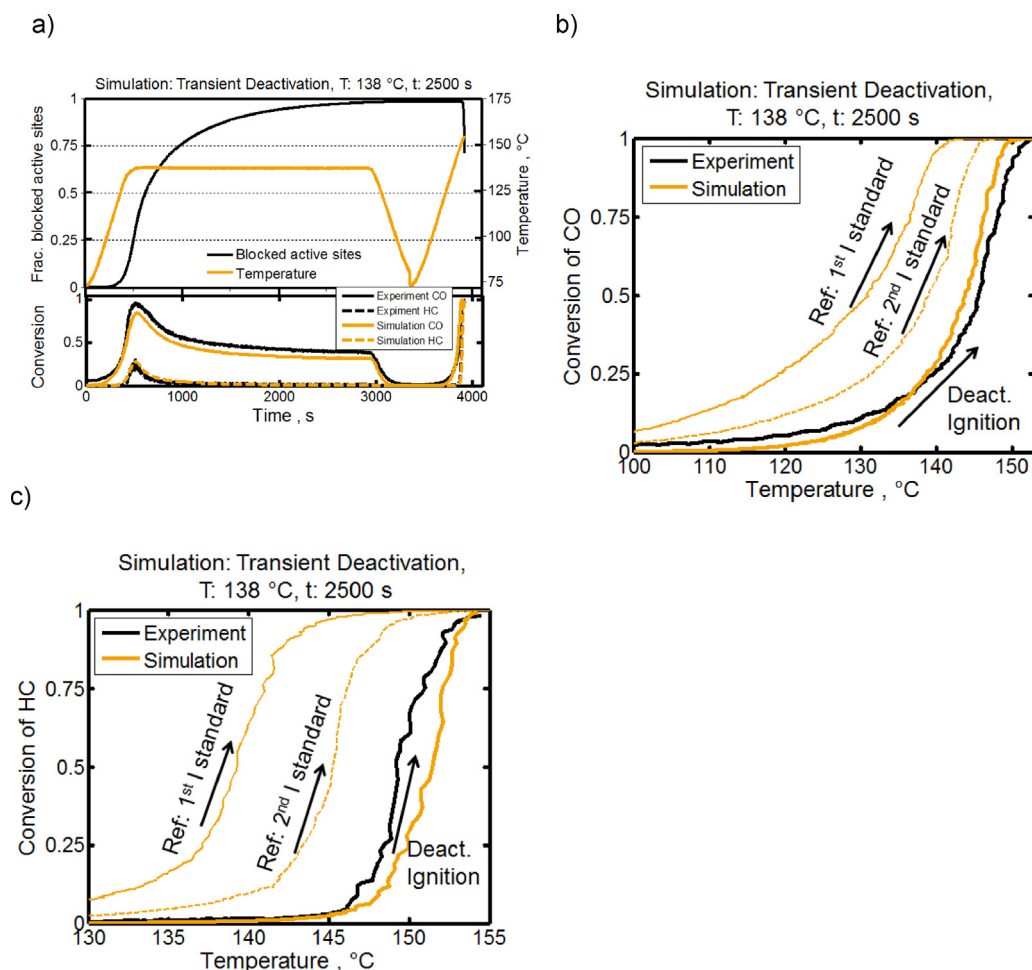


Fig. 12. Simulation of the transient deactivation experiment at 138 °C under standard conditions. a) The temperature ramps and the simulated fraction of blocked active sites A2* (average value over axial catalyst channel) for the transient deactivation experiment in the standard gas mixture at 138 °C followed by an extinction and an ignition branch. b) A comparison between the experimental and the simulated subsequent ignition curve for CO. The simulated first and the second experimental ignition curves of the standard experiment (see Fig. 1) are provided as references. c) the same as b) for C₃H₆.

The experiment as well as by the simulation meet this expectation for CO and C₃H₆ conversion. The maximum deviation between simulated and experimental data amounts 3 °C for CO and 2 °C for C₃H₆.

4. Conclusions

In this study we have demonstrated that in the presence of propene a Pt/Pd oxidation catalyst shows a deactivation that can be reversed by a treatment in a hydrocarbon free atmosphere. In the course of this study, a variety of different transient test protocols were applied to provide a detailed characterization of the hydrocarbon induced activation/deactivation effect, i.e. under which conditions the deactivation and the activation take place.

All the different experimental results of this paper can be consistently explained by a reversible blocking of the catalyst surface by propene partial oxidation products. In a typical light-off experiment, the HC deposits are first formed during the ignition branch, then are entirely removed at higher temperature after the HC ignition is completed and finally are formed again during the extinction branch, providing a deactivated state of the catalyst for the following ignition. This deactivation can be completely reversed either by a conditioning in an oxidizing exhaust mixture not containing any HC at a temperature of 110 °C or a conditioning in N₂ at a temperature of 140 °C.

More deposits can be formed during a slow heating ramp than during a fast heat-up, and this explains the fact that ignition temperature decreases with increasing ramp-rate, the opposite of what would be expected based on thermal considerations.

Constant temperature operation of the catalyst in the light-off range allowed a direct observation of the deactivation effect in the time domain.

All the experimental results could be nearly quantitatively described by a kinetic model that besides the standard kinetics for CO and propene oxidation considered the formation of site blocking species by partial oxidation of propene, as well as the removal of the deposits by oxidation or thermal desorption. While the success of this modeling exercise does not exclude other potential explanations of the hydrocarbon induced activation/deactivation phenomenon, it at least demonstrates that the proposed mechanism provides a consistent explanation for the experimental data. However, since no deactivation is observed if propene is omitted from the gas composition and in combination with previous direct observations of accumulating propene partial oxidation products by DRIFTS measurements [13,17,18], the results of this paper provide strong evidence that the demonstrated activation/deactivation effects can be attributed to a site blocking by propene oxidation intermediates.

In addition to already well established reversible activation/deactivation phenomena like the oxidation and reduction of Pt

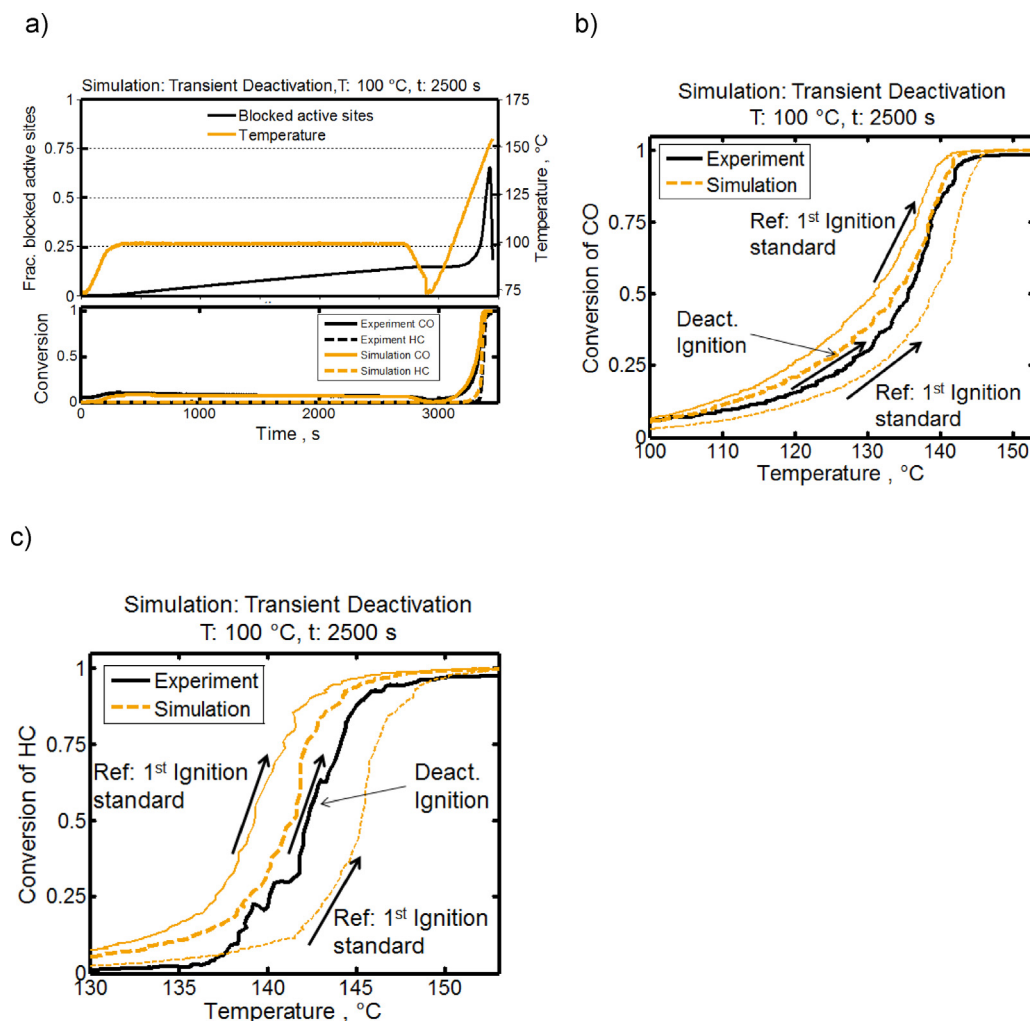


Fig. 13. Simulation of the transient deactivation experiment at 100 °C under standard conditions. The temperature ramps and the simulated fraction of blocked active sites $A2^*$ (average value over axial catalyst channel) for the transient deactivation experiment in the standard gas mixture at 100 °C followed by an extinction and an ignition branch are depicted in a). A comparison between the experimental and the simulated subsequent ignition curve are depicted in b) for CO and in c) for C3H6. The simulated first and the second ignition of the standard experiment are provided as references.

and PtO_x respectively, the formation of HC intermediates presents a further activation/deactivation effect that occurs under typical exhaust aftertreatment operating conditions. Such effects pose fundamental challenges for catalyst simulation and testing since due to the reversible deactivation effects, catalyst performance becomes a function of the operation history and not only of the current operating conditions. Simple test procedures may provide misleading results since they do not probe the catalyst in a state relevant under real operating conditions. Currently applied simulation approaches do not capture catalyst deactivation/activation effects.

To judge the impact of reversible deactivation effects during testing, simulation and practical applications of catalytic converters, it is important to obtain a detailed understanding of the underlying deactivation mechanisms. While in the current work, the deactivation effects caused by propene could be well described by a relatively simple model, one needs to be aware that real exhaust contains a multitude of different hydrocarbons which each might have a different impact on the catalyst activity. Experimental identification of all these contemporaneously occurring effects is an ambitious task. It is therefore important to be aware of the fundamental limitations of current kinetic modeling approaches.

Appendix A. Supplementary data

Supplementary data associated with this article can be found, in the online version, at <http://dx.doi.org/10.1016/j.apcatb.2017.08.026>.

References

- [1] J. Etheridge, T. Watling, The effect of Pt: Pd ratio on light-duty diesel oxidation catalyst performance: an experimental and modelling study, *SAE Int. J. Eng.* 8 (2015) (2015-01-1053).
- [2] B. Shakya, B. Sukumar, Y. López-De Jesús, P. Markatou, The effect of Pt: Pd ratio on heavy-duty diesel oxidation catalyst performance: an experimental and modelling study, *SAE Int. J. Engines* 8 (2015) (2015-01-1052).
- [3] J. Andersson, M. Antonsson, L. Eurenus, E. Olsson, M. Skoglundh, Deactivation of diesel oxidation catalysts: vehicle-and synthetic aging correlations, *Appl. Catal. B: Environ.* 72 (2007) 71–81.
- [4] J. Clerc, Catalytic diesel exhaust aftertreatment, *Appl. Catal. B: Environ.* 10 (1) (1996) 99–115.
- [5] W. Hauptmann, M. Votsmeier, J. Gieshoff, A. Drochner, H. Vogel, Inverse hysteresis during the NO oxidation on Pt under lean conditions, *Appl. Catal. B: Environ.* 93 (2009) 22–29.
- [6] K. Hauff, U. Tuttlies, G. Eigenberger, U. Nieken, Platinum oxide formation and reduction during NO oxidation on a diesel oxidation catalyst—experimental results, *Appl. Catal. B: Environ.* 123–124 (2012) 107–116.
- [7] K. Hauff, H. Dubbe, U. Tuttlies, G. Eigenberger, U. Nieken, Platinum oxide formation and reduction during NO oxidation on a diesel oxidation catalyst—macrokinetic simulation, *Appl. Catal. B: Environ.* 129 (2013) 273–281.

- [8] K. Hauff, W. Boll, S. Tischer, D. Chan, U. Tuttlies, G. Eigenberger, O. Deutschmann, U. Nieken, Macro- and microkinetic simulation of diesel oxidation catalyst: effect of aging, noble metal loading and platinum oxidation, *Chem. Ing. Tech.* 85 (2013) 673–685.
- [9] H. Dubbe, F. Bühner, G. Eigenberger, U. Nieken, Hysteresis phenomena on platinum and palladium-based diesel oxidation catalysts (DOCs), *Emission Control Sci. Technol.* 2 (3) (2016) 137–144.
- [10] A. Arvajová, P. Koci, V. Schmeißer, M. Weibel, The impact of CO and C₃H₆ pulses on PtO_x reduction and NO oxidation in a diesel oxidation catalyst, *Appl. Catal. B: Environ.* 181 (2016) 644–650.
- [11] A. Güthenke, D. Chatterjee, M. Weibel, B. Krutzsch, P. Koci, M. Marek, I. Nova, E. Tronconi, Current Status of modelling lean exhaust gas aftertreatment catalysis, *Adv. Chem. Eng.* 33 (2007) 103–211.
- [12] S. Voltz, C. Morgan, D. Liederman, S. Jacob, Kinetic study of carbon monoxide and propylene oxidation on platinum catalysts, *Ind. Eng. Chem. Prod. Res. Dev.* 12 (4) (1973) 294–301.
- [13] M. Khosravi, A. Abedi, R.E. Hayes, W. Epling, M. Votsmeier, Kinetic modelling of Pt and Pt: Pd diesel oxidation catalysts, *Appl. Catal. B: Environ.* 154 (2014) 16–26.
- [14] M. Herrmann, S. Malmberg, A. Drochner, H. Vogel, R. Hayes, M. Votsmeier, HC-induced deactivation in CO conversion at diesel oxidation catalysts, *Emission Control Sci. Technol.* 2.4 (2016) 181–187.
- [15] B. Bantl-Konrad, M. Weibel, B. Krutzsch, A. Massner, U. Gärtner, Realabgasuntersuchungen und detaillierte experimentelle Untersuchungen zum Einfluss von CO auf die NO₂-Bildung, FAD Konferenz Dresden (2012) (presentation).
- [16] A. Abedi, R. Hayes, M. Votsmeier, W. Epling, Inverse hysteresis phenomena during CO and C₃H₆ oxidation over a Pt/Al₂O₃ catalyst, *Catal. Lett.* 142 (2012) 930–935.
- [17] M. Hazlet, W. Epling, Spatially resolving CO and C₃H₆ oxidation reactions in a Pt/Al₂O₃ model oxidation catalyst, *Catal. Today* 267 (2016) 157–166.
- [18] M. Hazlet, M. Moses-Debusk, J. Parks, L. Allard, W. Epling, Kinetic and mechanistic study of bimetallic Pt-Pd/Al₂O₃ catalysts for CO and C₃H₆ oxidation, *Appl. Catal. B: Environ.* 202 (2017) 400–417.
- [19] W. Hauptmann, M. Votsmeier, H. Vogel, D. Vlachos, *Appl. Catal. A* 397 (2011) 174–182.
- [20] R. Raj, M. Harold, V. Balakotaiah, Steady-state and dynamic hysteresis effects during lean co-oxidation of CO and C₃H₆ over Pt/Al₂O₃ monolithic catalyst, *Chem. Eng. J.* 281 (2015) 322–333.
- [21] S. Oh, J. Cavendish, Transients of monolithic catalytic converters. Response to step changes in feedstream temperature as related to controlling automobile emissions, *Ind. Eng. Chem. Prod. Res. Dev.* 21 (1) (1982) 29–37.
- [22] M. Herrmann, PHD-Thesis: Reaktionstechnische Und Kinetische Untersuchung Des Diesel-Oxidations-Katalysators: Experiment Und Simulation, 2017.